

The *XMM-Newton* view of radio loud narrow line Seyfert1 galaxy PMN J0948+0022

Subir Bhattacharyya^{*}, Himali Bhatt, Nilay Bhatt and Krishna Kumar Singh

Astrophysical Sciences Division, Bhabha Atomic Research Centre, Mumbai 400085, India

ABSTRACT

We analysed the archival *XMM-Newton* data of radio loud narrow line Seyfert1 galaxy PMN J0948+0022 in the energy range 0.3–10.0 keV. The X-ray data revealed the spectrum in 0.3–10.0 keV energy band is not a simple power-law as described in literature. Instead it consisted of a power-law with soft excess below 2.5 keV. The X-ray spectrum was fitted with four different models and it was shown the soft excess component of the spectrum in 0.3–2.5 keV energy range could be described reasonably well within the framework of the thermal Comptonization model as well as relativistically blurred reflection model. The power-law component required to fit the spectrum beyond 2.5 keV was found to be rather hard compared to the ones observed in other obscured active galactic nuclei. It is also shown that the *Swift*/XRT spectrum from the source could not reveal the soft excess component due to poor statistics. The fractional variability estimated from *XMM-Newton* data indicates the presence of independently varying components in the spectrum above 1 keV.

Key words: extragalactic : Seyfert1 – X-ray – individual:PMN J0948+0022

1 INTRODUCTION

PMN J0948+0022 is a radio-loud narrow line Seyfert 1 (RLNLS1) galaxy, with cosmological redshift $z = 0.5846$ and radio loudness parameter $R \approx 846$ (Foschini 2011), detected in γ -rays by Large Area Telescope (LAT) on board *Fermi* satellite (Abdo et al. 2009b,a). It is also one of the six such sources detected by *Fermi*/LAT in the MeV–GeV region¹. Abdo et al.

^{*} E-mail:subirb@barc.gov.in

¹ <http://www.asdc.asi.it/fermi2lac/>

(2009b,a) reported the multi-wavelength observations of PMN J0948+0022 during March–July 2009, while Foschini et al. (2011) observed the source during a γ -ray outburst in July 2010. In both cases the observed spectral energy distribution (SED) looks very similar to the SED of typical high power blazars, known as flat spectrum radio quasars (FSRQs). The SEDs were modeled with the synchrotron and Comptonization models developed by Ghisellini & Tavecchio (2009). For both the observations the broadband SED were fitted with a synchrotron component for radio-to-IR/optical, a synchrotron self-Compton component for the X-rays, external Comptonization component for MeV–GeV γ -rays, and a thermal component from the accretion disk in the UV band. Interestingly, the fitted parameters and estimated power were found to fall in the region between the low power blazars (BL Lacs) and high power blazars (FSRQs). These derived properties are similar for other three *Fermi* observed RLNLS1 (Abdo et al. 2009a). Their analysis of broadband SED lead to similar conclusions. But the most intriguing fact is that the estimated black hole (BH) mass and mass accretion rates for RLNLS1, in terms of Eddington rate, are very different compared to those properties of blazars. The BH mass for RLNLS1 is approximately two orders of magnitude lower than the BH mass in blazars (Foschini 2011). Secondly, the RLNLS1s accrete at near Eddington limit, while blazars accrete at a much lower rate.

Here in this work, we gave a closer look at the X-ray spectrum of PMN J0948+0022. The reason is the following. In the broadband SED modelling for all γ -ray loud RLNLS1 the X-ray component is described by synchrotron self-Compton emission process (Abdo et al. 2009b,a). The X-ray spectra of radio quiet narrow line Seyfert 1 galaxies, as observed with *XMM-Newton*, show the presence of soft excess in the 0.3–2.0 keV energy band and a power-law component (Bian & Zhao 2004; Boller et al. 2003; Fabian et al. 2004; Haba et al. 2008; O’Brien et al. 2001; Page et al. 2003; Dewangan et al. 2007). The origin of the soft excess is not properly understood yet. In fact some of radio emitting NLS1 which are not categorized as radio-loud, also show strong soft excess in their X-ray spectrum, e.g, PKS 0558–504 (Papadakis et al. 2010). PKS 2004–447, another radio-loud ($R = 6358$) NLS1 (Foschini 2011), also show strong soft excess in its X-ray spectrum (Gallo et al. 2006). But there are some doubts about the classification of the source PKS 2004–447 (Oshlack et al. 2001). If the X-ray spectrum of γ -ray loud RLNLS1 PMN J0948+0022 also show the presence of soft excess then it is important to understand their origin as well as their connection to the γ -ray emission. Here, we discussed the analysis and modelling of archival data of PMN J0948+0022 observed with *XMM-Newton*, *Swift*/XRT to show that the X-ray spectrum of the source has

a complex structure and *Swift*/XRT can not adequately describe it. We also analysed the *Fermi*/LAT data taken simultaneously with *XMM-Newton* observation to study the γ -ray emission from PMN J0948+0022.

The paper is structured as follows. In section 2, we described the data reduction for *XMM-Newton*, *Swift*/XRT and *Fermi*. The spectral modelling is described in section 3, results are discussed and concluded in sections 4 and 5, respectively.

2 DATA REDUCTION

2.1 *XMM-Newton* observations

PMN J0948+0022 was observed by *XMM-Newton* telescope (for details see Strüder et al. (2001); Turner et al. (2001)) operated with Medium filter at two epochs during April, 2008 (Observation ID 0502061001, hereafter Obs-A) and May, 2011 (Observation ID 0673730101, hereafter Obs-B) for approximately 24 ks and 93 ks, respectively. The X-ray data is not taken in prime full window mode for EPIC-MOS detectors (MOS1 and MOS2; Turner et al. (2001)) for Observation ID 0502061001 *and the source was not available within the CCD frame*, therefore, only EPIC-PN (European Photo Imaging Camera; Strüder et al. (2001)) data were used for further analysis. For Obs-B, the total observation time intervals of MOS detectors were split into five short duration segments of 16 ks (M1), 28 ks (M2), 25 ks (M3), 4 ks (M4), 10 ks (M5), however, the data have been taken for full observation time span, i.e. 93 ks, for PN detector.

2.1.1 EPIC data

Data reduction followed standard procedures using *XMM-Newton* Science Analysis System software (SAS version SAS11.0.0) with updated calibration files. Event files for the MOS (*for Obs-B*) and the PN (*for Obs-A and Obs-B*) detectors were generated using the tasks EMCHAIN and EPCHAIN, respectively. These tasks allow calibration of the energy and the astrometry of the events registered in each CCD chip and to combine them in a single data file. Event list files were extracted using the SAS task EVSELECT. Data from the three cameras were individually screened for the time intervals with high background when the total count rate (for single events of energy above 10 keV) in the instruments exceed 0.35 and 1.0 counts s⁻¹ for the MOS and PN detectors respectively.

Source photons were extracted from circular region of 40'' around the source position to

generate the light curves and spectra. Background was estimated from a number of empty regions close to the X-ray source in the detector. X-ray spectra and light curves of the source were generated using SAS task EVSELECT and background scaling factor have been calculated using BACKSCALE task. The photon redistribution as well as the ancillary matrix were computed using SAS task RMFGEN and ARFGEN. Finally, the PN spectra of Obs-A and Obs-B were rebinned to have at least 20 and 80 counts per bin respectively while the MOS1 and MOS2 spectra of Obs-B were rebinned to have at least 20 counts per spectral bin.

2.2 *Swift* observations

X-ray data from X-ray telescope (XRT) on *Swift* have also been analysed here in photon counting mode. These observations have been taken on the same date as for Observation ID 0673730101 from *XMM-Newton*, i.e., 28 May 2011. The *Swift*/XRT data has been reduced using the HEASoft packages (6.12 version), including XSELECT, XIMAGE, and *Swift* data analysis tools. The XRT tool XRTPipeline is used to produce the clean event data. X-ray spectra were extracted using XSELECT with 20 pixel radius source extraction region and background region from clean event data. Response matrices files (RMF) and Ancillary Response Files (ARFs) were generated from task XRTMKARF using the CALDB version 014 (released date 25 July 2011). Finally, the spectra were grouped using the GRPPHA task with 20 counts per bin.

2.3 *Fermi*/LAT observation

The Large Area Telescope(LAT), onboard *Fermi* gamma-ray observatory, is a pair conversion detector (Atwood et al. 2009). It is sensitive to the gamma-rays in the energy range ~ 20 MeV to >300 GeV with peak effective area of ~ 8000 cm² at 1 GeV. LAT has a very wide field of view of 2.4 sr covering 20% of the sky at any instant with angular resolution of ~ 1 deg. at 1 GeV.

The LAT data for the source considered for the present analysis cover the period May 15–June 15, 2011. The data have been analyzed using the standard *Fermi*-LAT ScienceTools software package (ver. v9r27p1)² and with the help of the analysis threads and other doc-

² <http://fermi.gsfc.nasa.gov/ssc/data/analysis/software/>

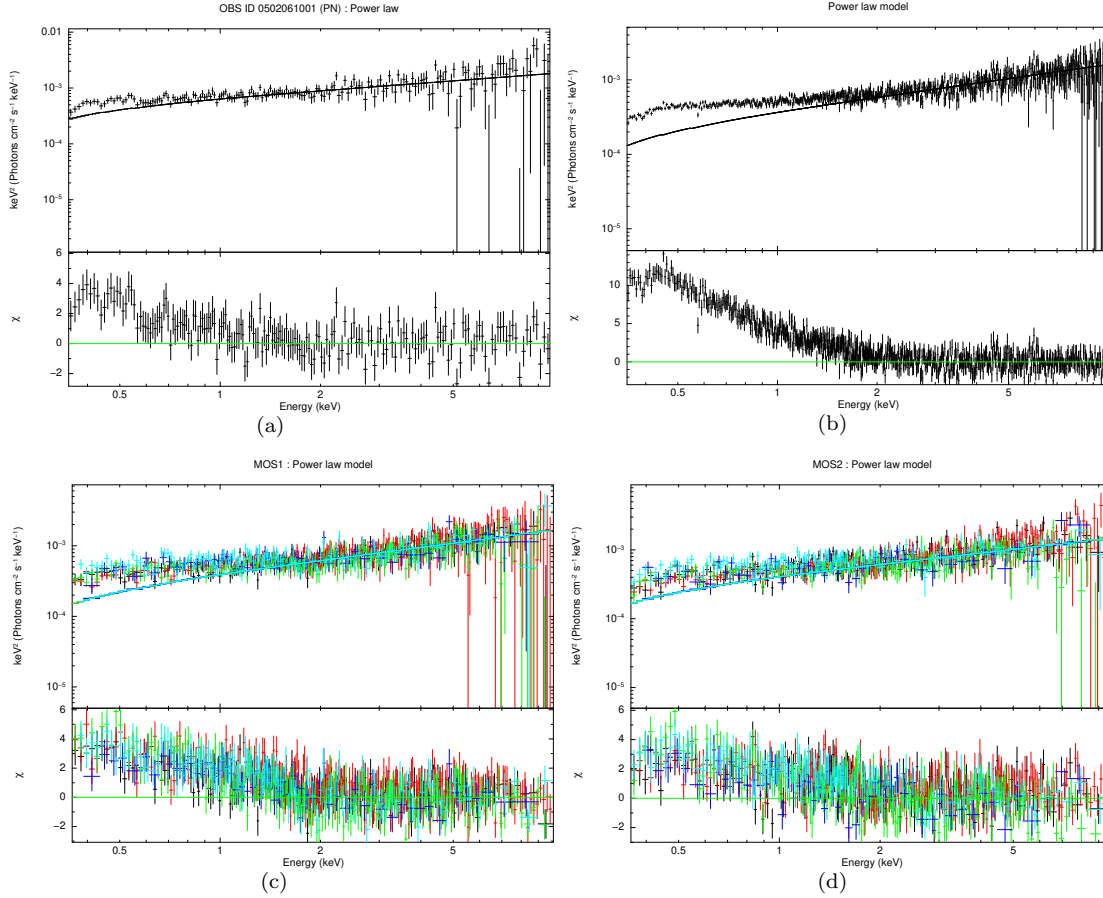


Figure 1. Soft excess is shown for (a) EPIC-PN spectrum for Obs-A, (b) EPIC-PN, (c) MOS1 and (d) MOS2 spectra for Obs-B. The power-law model is fitted for the energy range 2.5 keV and above in each case.

umentation available at *Fermi* Science Support Center webpages³. We have selected only "Diffuse" class events (i.e. the purest gamma-ray events) in the energy range 100 MeV to 300 GeV within 10° region of interest (ROI) centered around the source position (RA = 09^h48^m57^s.3 and Dec = +00°22'25".6) using GTSELECT task. In order to avoid background contamination from the bright Earth limb, we have discarded photons arriving from zenith angle greater than 105°. We selected only those time intervals during which the events/photons qualify for science analysis using the filter expression (DATA_QUAL==1 && LAT_CONFIG==1 && ABS(ROCK_ANGLE)<52) within GTMKTIME task. Then the livetime for the source was calculated and exposure map of the source was generated. Finally, using Unbinned likelihood analysis tool (GTLIKE), we fitted the source spectrum along with other 21 sources present within the ROI of 10° centered around PMN J0948+0022 and obtained the flux in the energy band 100 MeV – 300 GeV. For this we created source model

³ <http://fermi.gsfc.nasa.gov/ssc/data/analysis/>

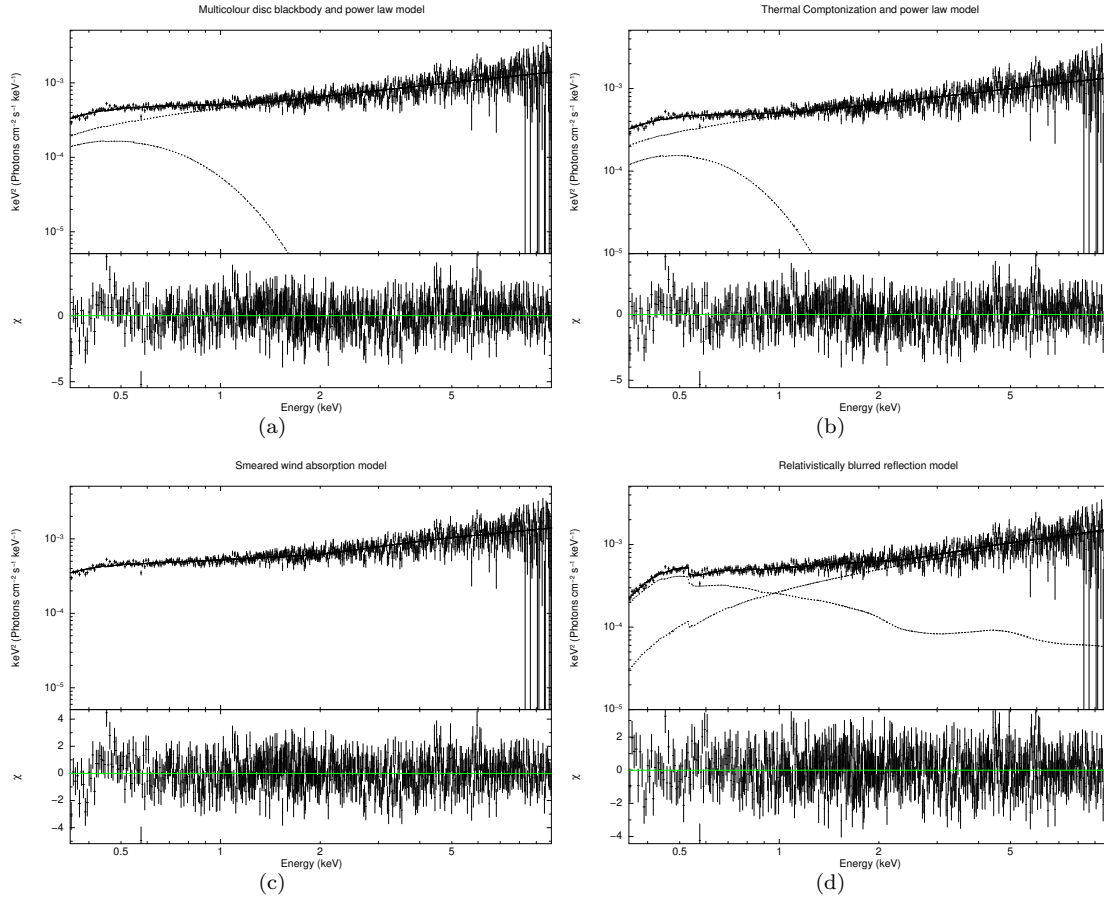


Figure 2. EPIC-PN X-ray spectrum of Obs-B with best fit models : (a) Multicolour blackbody with power-law, (b) Thermal Comptonization and power-law, (c) Smeared wind absorption model and (d) Relativistically blurred reflection model. χ^2 distributions of fitting are given in lower panels of each plot.

file containing model spectra for all these 21 gamma-ray sources visible in the ROI as listed in the 2nd *Fermi*/LAT catalogue and diffuse emission models of galactic and extragalactic origins. For PMN J0948+0022, we have taken power-law spectrum model. We obtained the value of test statistics (TS; detection significance of the source $\approx \sqrt{TS}$) as 32.86 for the whole energy range 100 MeV–300 GeV.

3 RESULTS

3.1 Spectral analysis

The EPIC-PN spectra of both the observations and MOS1 and MOS2 spectra of Obs-B were fitted with a power-law distribution with the photon index Γ using the spectral modelling tool XSPEC (Arnaud 1996). The power-law is modulated by the galactic absorption. The complete photon spectra for both the observations in the 0.35–10.0 keV energy range could not be fitted well with the power-law and galactic absorption model. On the other hand the

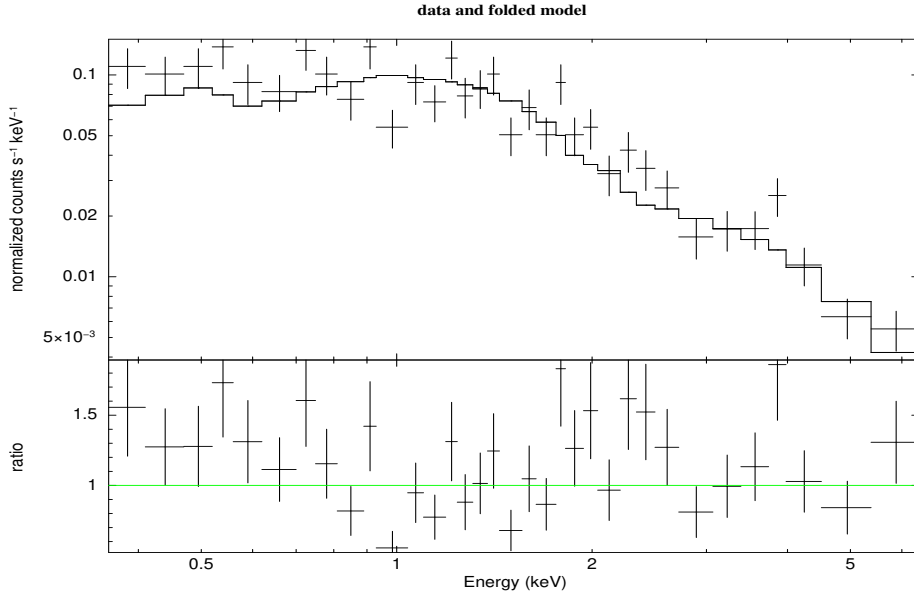


Figure 3. *Swift*/XRT spectrum with best-fit model ZWABS*ZPOWERLAW

spectra were fitted well by a power-law in the energy range 2.5–10.0 keV. The photon indices were found to be 1.35 ± 0.15 , 1.37 ± 0.04 , 1.38 ± 0.06 and 1.45 ± 0.06 for PN spectrum (Obs-A), PN spectrum (Obs-B), MOS1 (Obs-B) and MOS2 (Obs-B) spectra respectively. The χ^2/dof values are 73.20/66 (PN, Obs-A), 335.49/312 (PN, Obs-B), 274.6/324 (MOS1, Obs-B) and 388.13/302 (MOS2, Obs-B). The power-law component when extended to lower energies (upto 0.35 keV) revealed a soft excess in the 0.35–2.5 keV energy range. The presence of soft excess component in the PN and MOS spectra are shown in Fig 1.

Even though the soft excess in X-rays is seen case of narrow line Seyfert galaxies and it is one of the most important components of AGN spectra, its origin is still not well understood. Different physical models have been used to describe the soft excess component, such as, (i) the multicolour blackbody radiation from the disc (Mitsuda et al. 1984; Makishima et al. 1986), (ii) thermal Comptonization model (Titarchuk 1994), (iii) smeared wind absorption model (Gierliński & Done 2004) and (iv) relativistically blurred reflection model (Ross & Fabian 2005). Here we use all four models to understand the soft excess component in X-ray spectrum of PMN J0948+0022. The merits and demerits of these models are discussed in the next section to choose the best plausible model.

Before using the physical models, we used phenomenological model broken power-law to get an idea of the relative steepness of the soft and hard components of the spectrum. The fitting of PN spectrum of Obs-B with a broken power-law yielded photon indices 1.92 ± 0.01 and 1.46 ± 0.02 below and above the break energy at 1.68 ± 0.02 keV. The χ^2/dof came out

to be 843.7/697. With this estimations of the photon indices we applied different physical models to fit the PN spectrum.

Multicolour disc blackbody and power-law

Considering the fact that the soft excess is contributed by the accretion disc of the galaxy around the central black hole, we fitted the spectrum with spectral models multicolour disc blackbody and a power-law. The complete spectral model used was ZWABS*(DISKBB+ZPOW). The equivalent hydrogen column density used to account the galactic absorption was fixed at $4.4 \times 10^{20} \text{ cm}^{-2}$ (Kalberla et al. 2005). The power-law photon index (Γ) was 1.53 ± 0.02 indicating a hard power-law and the inner disc temperature was found to be $162 \pm 6 \text{ eV}$. The spectral fit was reasonably good with $\chi^2/dof = 827.45/693$ and the fitted spectrum with its residual is shown in Figure 2. The disc temperature obtained here was much higher than the inner disc temperature expected for an accretion disc around a black hole (BH) of mass $3 \times 10^7 M_{\odot}$ which is the mass of the BH estimated by Yuan et al. (2008).

Thermal Comptonization of disc photons

The other possibility could be that the seed photons originating from the accretion disc were Compton boosted by thermal electrons in an optically thick corona to produce the soft excess. We have used ZWABS, COMPTT - the thermal Comptonization model and a power-law component ZPOW to fit the complete spectrum. Considering the fact that the corona temperature $\sim 0.150 \text{ keV}$ (as obtained for inner disc temperature in case of multicolour disc blackbody spectrum) and power-law photon index $\Gamma \sim 1.9$ (as obtained for the steeper component of the power-law in the phenomenological broken power-law model) the plasma optical depth (τ) could be estimated from the relation (Sunyaev & Titarchuk 1980)

$$\Gamma - 1 = \left[\frac{9}{4} + \frac{\pi^2}{3} \frac{1}{\left(\frac{kT_e}{mc^2}\right) \left(\tau + \frac{2}{3}\right)^2} \right]^{\frac{1}{2}} - \frac{3}{2} \quad (1)$$

where kT_e is the electron temperature and Γ is the photon index. This brought out the optical depth ~ 52 . With the seed photon temperature at 30 eV and the equivalent hydrogen column density was fixed at $4.4 \times 10^{20} \text{ cm}^{-2}$ (Kalberla et al. 2005) the complete spectrum was fitted using the model ZWABS*(COMPTT+ZPOW). The fitted value of electron temperature was $0.187_{-0.009}^{+0.008} \text{ keV}$ and that of photon index was 1.55 ± 0.02 . The value of χ^2/dof is 834.67/697.

Smearred wind absorption model

Gierliński & Done (2004) discussed the relativistic smearing of characteristic atomic absorption features in a moderately relativistic wind/outflow from the inner accretion disc to explain the soft excess in the X-ray spectrum of Seyfert 1 galaxies. The main parameters of the model are the absorption column density, ionization parameter (ξ) and velocity dispersion (σ) of the Gaussian velocity distribution of the wind. Model is described by SWIND1 within XSPEC. The model SWIND1 along with the photo-electric absorption ZWABS and the power-law for the background continuum gives $\chi^2/dof = 809.98/692$ with the present data from EPIC-pn. The fitted parameters are - the absorption column density : $> 25.2 \times 10^{22}$ cm^{-2} , the ionization parameter : 3.44 ± 0.12 and the velocity dispersion $\sigma > 0.5$ (in the unit of $\frac{v}{c}$) and the photon index is 1.71 ± 0.02 .

Relativistically blurred reflection model

In this model the cold optically thick accretion disc is illuminated by a power-law distributed radiation and the accretion disc medium produces a Compton scattered reflected radiation along with fluorescence lines. The resultant emission involves the reflected component from the disc and the illuminating power-law. The relativistic blurring of resultant emission is accounted for by convolving a Laor (1991) profile used to simulate the blurring emission lines from an accretion disc around a maximally rotating black hole. The Laor profile estimation considers that the accretion disc is geometrically thin, flat and has well defined inner and outer radius. The radial dependence of disc emissivity is assumed to be a power-law. This model was first introduced by Ross & Fabian (1993) and used by Ballantyne et al. (2001a), Ballantyne et al. (2001b), Fabian et al. (2002) and Ballantyne et al. (2003). It was further updated by including more ionization states and more atomic data by Ross & Fabian (2005). The updated model by Ross & Fabian (2005) was successfully used by Crummy et al. (2006) and Walton et al. (2012) for a large sample of AGN while by Nardini et al. (2011) for AGN Ark 120. The parameters of the model are inner and outer radii of the accretion disc, iron abundance of the gas, spectral index of illuminating power-law radiation, emissivity index of the disc, ionization parameter and the inclination of the disc. The fitting of the source spectrum in the 0.35–10.0 keV energy band requires an additional local absorption due to the warm absorber apart from the galactic absorption. The final model used for the fitting was `WABS*ZWABS*KDBLUR(POWERLAW + ATABLE{REFLIONX.MOD})`. The equivalent hy-

drogen column density was kept fixed at $4.4 \times 10^{20} \text{ cm}^{-2}$ (Kalberla et al. 2005) while the equivalent hydrogen column density corresponding to the local warm absorber was fitted to $8.0_{-2.0}^{+4.0} \times 10^{20} \text{ cm}^{-2}$. The fitted value of the inner radius of the accretion disc was $1.49_{-0.13}^{+0.21} r_g$ where r_g is the gravitational radius of the black hole. The inner radius value was very close to the inner most stable circular orbit around a maximally rotating Kerr black hole. We obtained the lower limit ~ 6 of the emissivity index for the disc. The power component came out to harder as compared to the other models used here. The photon index of the power-law component was fitted to 1.30 ± 0.06 . The REFLIONX component had disc iron abundance $0.21_{-0.05}^{+0.14}$, ionization parameter $2000.0_{-947.4}^{+1472.2}$ and illuminating radiation photon index $2.70_{-0.06}^{+0.17}$. The fitted spectrum along with the residual is given in Figure 2. The fitted parameters for all four models are given in Table 1.

Even though the above discussions were based on the EPIC-PN spectrum of Obs-B, we also fitted the EPIC-PN spectrum of Obs-A and MOS1 and MOS2 spectra of Obs-B with the above models. The fitted parameter values were generally consistent, but the error bars were large.

Swift/XRT spectrum

We fitted the XRT data with model ZWABS*ZPOW. The galactic absorption and power-law model fitted, but due to poor statistics of the data the soft excess in the spectrum could not be detected. In fact the fitting was also not of that good quality yielding $\chi^2/\text{dof} = 62.04/32$. The fitted spectrum is shown in Figure 3 and the best-fit parameters are given in Table 1.

3.2 Spectral variability

The lightcurves with 500 s time bin, in the 0.35–2.50 keV and 4.0–10.0 keV energy bands, and the corresponding hardness ratio are shown in Figure 4a. Following Vaughan et al. (2003a) we also calculated the fractional variability (F_{var}) for the lightcurves in the energy bands 0.3–0.8 keV at the step of 0.1 keV, 0.8–1.0, 1.0–2.0, 2.0–3.0 and 3.0–5.0 keV. The rms spectrum is shown in Figure 4b. The fractional variability did not vary significantly up to 1 keV and remained around 10%. Beyond 1 keV F_{var} showed a trend of increase and reached up to 20%.

We used 100 sec binned lightcurves for the energy ranges 0.3–2.5 keV, 4.0–10.0 keV and for the complete energy range 0.3–10.0 keV to calculate the rms amplitude of variability (σ_{rms}).

Parameters	Best-fit values
<i>XMM-Newton</i> (0673730101) : PN	
Model	ZWABS*(DISKBB + ZPOWERLAW)
T_{in} (keV)	0.162 ± 0.006
N_{diskbb}	$44.29^{+8.09}_{-5.99}$
Γ_{pl}	1.529 ± 0.016
N_{pl}	$9.53^{+0.22}_{-0.21} \times 10^{-4}$
χ^2/ν	827.45/693
Model	ZWABS*(COMPTT + ZPOWERLAW)
T_0 (keV)	3.0×10^{-2}
kT_e (keV)	$0.187^{+0.008}_{-0.009}$
N_{compTT}	$1.11^{+0.15}_{-0.13} \times 10^{-2}$
Γ_{pl}	1.55 ± 0.02
N_{pl}	$9.93^{+0.30}_{-0.29} \times 10^{-4}$
χ^2/ν	834.67/693
Model	ZWABS*SWIND1*ZPOWERLAW
col. dens. ($\times 10^{22}$ cm $^{-2}$)	> 25.2
$\log \xi$	3.44 ± 0.12
σ (in units of v/c)	> 0.2
Γ_{pl}	1.71 ± 0.02
N_{pl}	$1.77 \pm 0.04 \times 10^{-3}$
χ^2/ν	809.98/692
Model	WABS*ZWABS*KDBLUR(POWERLAW+ATABLE(REFLIONX.MOD))
col. dens. ($\times 10^{22}$ cm $^{-2}$)	$0.08^{+0.04}_{-0.02}$
Index	> 5.77
Rin(G)	$1.49^{+0.21}_{-0.13}$
Inclination (deg)	$74.22^{+2.03}_{-14.16}$
Fe/solar	$0.21^{+0.15}_{-0.05}$
Gamma	$2.70^{+0.17}_{-0.07}$
Xi	2000^{+1472}_{-947}
$N_{reflionx}$	$1.43^{+1.64}_{-0.71} \times 10^{-8}$
Γ_{pl}	$1.30^{+0.06}_{-0.06}$
N_{pl}	$3.21 \pm 0.32 \times 10^{-4}$
χ^2/ν	760/692
<i>Swift</i> (00031306014) : XRT	
Model	ZWABS*ZPOWERLAW
Γ_{pl}	1.58 ± 0.11
N_{pl}	$2.55 \pm 0.17 \times 10^{-3}$
χ^2/ν	62.04/32

Table 1. The best-fit values of the spectral parameters derived from spectral fitting of X-ray data with different models using χ^2 minimization technique.

The rms amplitude of variability for a lightcurve with N data points and mean count rate \bar{x} is given by (Uttley et al. 2005)

$$\sigma_{rms} = \sqrt{\frac{1}{N-1} \sum_{i=1}^N (x_i - \bar{x})^2}. \quad (2)$$

The length of each segment of the lightcurve considered was 2000 sec. The variation of the calculated rms variability with the mean count rate for the all three energy ranges are shown Figure 5. It is evident that, within the limited dynamical range of the count rate, the flux vs σ_{rms} follows a linear relationship. This is true for the lightcurves in all three energy

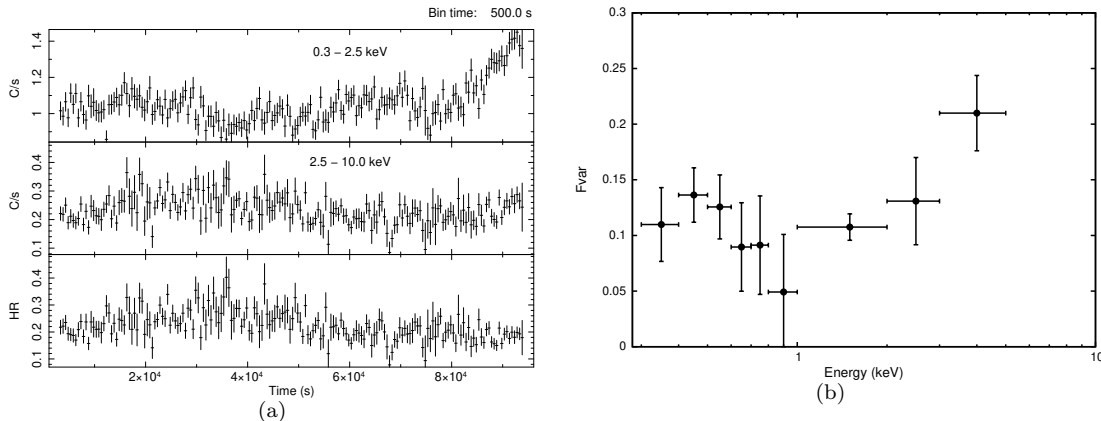


Figure 4. (a) Lightcurve for 0.3–2.5 keV (S), 2.5–10 keV (H) and the corresponding hardness ratio (H/S); (b) rms spectrum as obtained from *XMM-Newton* observation (Obs-B)

segments. The distribution of points are fitted with linear equations with slopes 10.53 ± 0.58 (for 0.3–2.5 keV band) and 10.76 ± 1.41 (for 4–10 keV band).

4 DISCUSSION

To understand the spectral behaviour of radio-loud narrow line Seyfert 1 galaxy PMN J0948+0022 in the X-ray energy band we analysed the archival data of the source from *XMM-Newton*. The EPIC-PN spectrum of the source in 0.3–10.0 keV region could not be fitted with a simple power-law. The spectrum in the 2.5–10.0 keV energy range fits reasonably well with a power-law distribution ($\chi^2/\text{dof} = 335.5/310$) with spectral index 1.37 ± 0.03 while the data in the 0.3–2.5 keV energy range show the presence of a distinct soft excess component when compared with the power-law extrapolated from the high energy. The soft excess is commonly observed in case of radio-quiet as well as radio-loud narrow line Seyfert 1 galaxies, but in the present context it has different importance. Since PMN J0948+0022 is a gamma-ray emitter which establishes the existence of powerful jet in the system, so it is not only important to understand the origin of the soft excess in the X-ray domain, it is also very crucial to understand its connection with the gamma-ray emission. The latter may shed some light on the disc-jet connection which is not well understood in the theory of accretion and jet formation, even after a lot work have already been done in this area (e.g, Neilsen & Lee (2009)).

Due to the uncertainties in the understanding of the soft excess in the X-ray spectrum of NLS1, we considered four different models to fit the EPIC-pn spectrum of PMN J0948+0022.

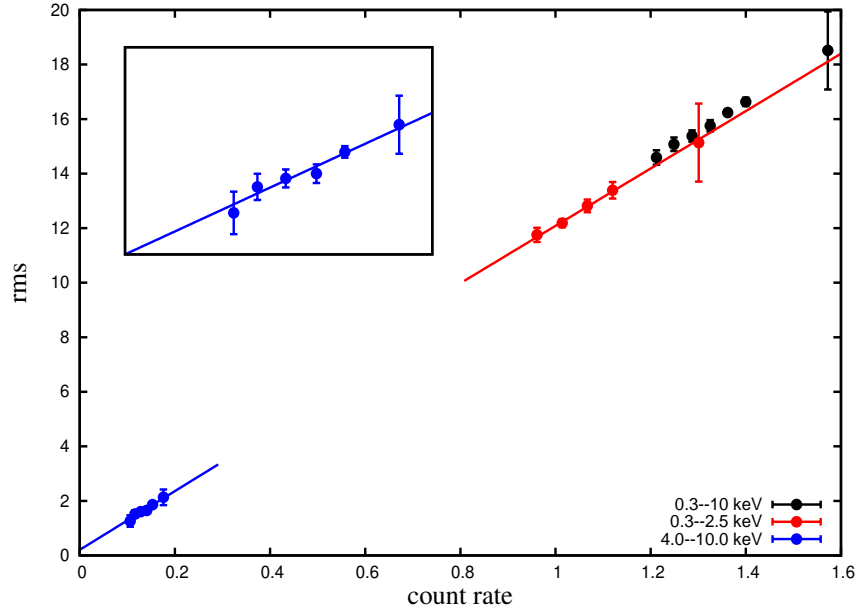


Figure 5. rms–count rate correlation for *XMM-Newton* data in the frequency range, $5 \times 10^{-4} - 5 \times 10^{-2}$ Hz ; *red*: 0.3–2.5 keV, *blue*: 4–10 keV POWERLAW component, *black*: 0.3–10.0 keV. Same coloured lines are the best-fit functions for the respective data sets. *inset*: zoom-in of the POWERLAW component

Among the models used here it is very difficult to rule out any of them just by considering the value of χ^2/dof .

The multicolour disc blackbody and power-law model give the inner disc temperature $\sim 0.162 \pm 0.006$ keV and a power-law index $\sim 1.528 \pm 0.016$. Yuan et al. (2008) estimated the black hole mass $\sim 10^{7.5} M_{\odot}$ for PMN J0948+0022. For such value of the BH mass the inner disc temperature of a standard accretion disc can not be as high as 0.162 keV. This fact essentially rules out the possibility that the multicolour disc blackbody can explain the observed soft excess.

In case of thermal Comptonization model, the soft excess in 0.35–2.50 keV energy range was modeled by the Comptonization of disc photons in an optically thick cold thermal corona. The characteristic photon temperature from the accretion disk was held fixed at 30 eV which is the typical inner disc temperature for an accretion disc around a black hole of mass $10^{7.5} M_{\odot}$. The fitted value of the corona temperature was found to be $0.187_{-0.008}^{+0.009}$ keV. The optical depth of the corona was fixed at 52. The fitting of the power-law component yielded a hard power-law with spectral index 1.48 ± 0.03 . This hard power-law component can be modeled by invoking a hot corona with moderate optical depth ($\tau \sim 1$). Such two corona scenarios were discussed in the literature in the context of explaining the X-ray spectra of Seyfert 1 galaxies (Zdziarski et al. 1996; Magdziarz et al. 1998; Dewangan et al. 2007; Laor et al. 1997). The seed photons for the cold optically thick corona are possibly the

photons from the accretion disc while the seed photons for the hot corona can be from the accretion disc *or* photons of the soft excess from the optically thick corona. To distinguish the possible origin of the seed photons in the hot corona, we studied the cross-correlation between the soft excess and power-law flux. It was found that there was no correlation between the two energy bands. If the soft excess photons served as the seed photons in the hot corona then there must be a correlation between the bands. Therefore, it was most likely that the disc photons of temperature 30 eV served as the seed photons in the Comptonizing hot corona and the power-law component was produced in this part of the corona only by the process of thermal Comptonization. The main problem of using this model as it was done in case of soft excess using the spectral model COMPTT was that the observed spectrum with *XMM-Newton* extends up to 10 keV only. It is noted that the observed spectrum does not show any cut-off at this energy. Due to the absence of any cut-off the temperature of the corona which determines the cut-off in the photon spectrum could not be constrained. The observation of the source in hard X-rays may reveal the thermal cut-off if the power-law was indeed produced by the thermal Comptonization. The X-ray flux obtained in the 0.35–10.0 keV energy range was 4.05×10^{-12} ergs cm⁻² s⁻¹. This led to a luminosity $\sim 3 \times 10^{45}$ erg s⁻¹ which, for a BH mass $\sim 10^{7.5} M_{\odot}$, is $0.6 L_{Edd}$.

The thermal origin of soft excess leads to a difficulty that the temperatures of the thermal electron required to fit the spectrum fall within a very narrow range (~ 0.1 – 0.3 keV) irrespective of the mass of the accreting black hole. Recently, Jin et al. (2012); Done et al. (2012) modeled the X-ray spectra of a large number of unobscured type 1 Seyferts using the thermal Comptonization model and it was found that the electron temperature varies from 0.1–0.6 keV while the black hole mass ranges from $\sim 10^6$ – $10^9 M_{\odot}$. Therefore, the values of electron temperature obtained here are generally consistent with same reported in the literature. Such a narrow temperature range and its independence on black hole mass suggest that the soft excess could have had atomic origin (Gierliński & Done 2004; Ross & Fabian 1993, 2005). We used the smeared wind absorption model by Gierliński & Done (2004) to fit the X-ray spectrum of the source. In this model, the power-law component is produced in the Comptonizing corona and the soft excess is produced due to the smeared atomic absorption features in soft X-rays (Gierliński & Done 2004). The smearing of absorption features takes place in differentially rotating mildly relativistic wind outflow/jet from the accretion disc. The fitting of the spectrum yielded an absorption wind column density $> 25 \times 10^{22}$ cm⁻², the ionization parameter is 3.44 ± 0.12 and the dispersion of Gaussian velocity distribution,

$\sigma > 0.5$. The value of σ implied that the outflow was mildly relativistic with Lorentz factor ≥ 1.2 . Therefore this model requires the launching of a relativistic outflow to fit the soft excess data.

The relativistically blurred reflection model which also considered the atomic origin of the soft excess, gave a reasonably good fit to the observed spectrum. The fitted value the inner radius not only implied a rapidly spinning black hole, it also implied that the emission region is situated in the innermost portion of the accretion disc. This also implied that the reflected radiation would have very blurring due to the gravitational field of the black hole. The illuminating radiation had steeper photon index compared to the hard power-law component in the spectrum. The hard power-law component might be produced in a corona in the outer portion of the disc as mentioned earlier. The estimated luminosity of the source came out to be 3.1×10^{45} ergs s⁻¹ which is approximately $0.6L_{Edd}$.

The other aspect of the present study is the study of rms spectrum. The calculated rms spectrum remained almost constant upto 1 keV and it increased beyond 1 keV. The beyond 1 keV there might be independently varying spectral components and the power spectral density could be energy dependent (Vaughan et al. 2003a). As the error bars are relatively large, so to draw any firm conclusion on spectral variability for photon energies beyond 1 keV longer observations are required.

The other important aspect of the emission from PMN J0948+0022 is the linear relation between the rms variability amplitude and the mean count rate. This feature is also seen in case of narrow line Seyfert 1 galaxies (Edelson et al. 2002; McHardy et al. 2004) and from Seyfert 1 galaxies (Vaughan et al. 2003c,b). Uttley et al. (2005) showed that the linear rms-flux relation is an outcome of a multiplicative process where the amplitude of short time-scale variations are modulated by the longer time scale variations. In case of accretion flow the long time scale variations are produced at larger radii whereas the short time scale variations are produced at shorter radii of the accretion disc. In fact Lyubarskii (1997) proposed a model where the fluctuations originated at the larger radii of the accretion disc were considered to propagate to smaller radii, to explain the observed X-ray variability in X-ray binaries. Uttley & McHardy (2001) showed that the linear relationship between the rms variability amplitude and flux is a natural outcome of the model proposed by Lyubarskii (1997).

Finally, in the 0.1–300 GeV energy range, *Fermi*/LAT detected γ -ray emission from the source. The analysis of the data for one month around the *XMM-Newton* observation (Obs-

B) discussed here, showed a gamma-ray flux of $(8.34 \pm 0.19) \times 10^{-8}$ photons $\text{cm}^{-2} \text{s}^{-1}$. Earlier the gamma-ray detection was reported by Abdo et al. (2009b); Foschini et al. (2010, 2012). The multiwavelength spectral data were modeled by using synchrotron process for the radio-to-optical band; X-ray and γ -ray spectra were fitted with self-synchrotron Compton and external Compton processes respectively. The radiation is produced in a region in relativistically moving jet. In those works the X-ray spectra were considered from *Swift*/XRT in the 0.2–10 keV band and the XRT spectra were fitted with simple power-law. But in the present work it is shown that the X-ray spectrum in the 0.2–10 keV energy band was not a power-law. The near simultaneous *Swift*/XRT data were analysed here and it was shown that the data could not reveal the soft excess component due to poor statistics. Therefore the consideration that the X-ray spectrum was a simple power-law and originated in a relativistic jet might be misleading. It indeed has a soft excess component from the accretion disc. This must be taken into account while modelling the multiwavelength spectral energy distribution. It is also important to understand the relationship between the soft excess component and the very high energy component of the spectrum which is beyond the scope of this paper.

5 CONCLUSIONS

We have analysed the archival X-ray data from *XMM-Newton*, *Swift*/XRT and γ -ray data from *Fermi*/LAT for the radio loud narrow line Seyfert 1 galaxy PMN J0948+0022. This conclude the following.

- The spectral analysis of X-ray spectrum from *XMM-Newton* establishes the presence of soft excess in the 0.3–2.5 keV energy band and a hard power-law beyond 2.5 keV.
- Due to the uncertainties in the understanding of the soft excess in the X-ray spectrum of NLS1 the complete spectrum is fitted with four different spectral models - (1) multicolour black body and power-law, (2) thermal Comptonization and power-law, (3) smeared absorption wind model and (4) the relativistically blurred reflection model. The models (1) and (3) are completely ruled out, but models (2) and (4) are statistically comparable to each other. Due to the fact that the temperature of the optically thick corona where the soft excess is produced by thermal Comptonization, falls in a very narrow range irrespective of the mass of the central black hole, the relativistically blurred reflection model is preferred.
- The simultaneous multi-wavelength fitting of the spectrum should take care of the soft

excess part of the spectrum properly. The power-law component in the X-ray spectrum might also be originated in the accretion disc corona. The SSC process might not be the correct description of X-ray emission in 0.3–10.0 keV energy range. It is also important to understand the possible connection between the soft excess and the gamma-ray emission in the source.

- It is important to study the variability properties of this source in detail. This study will be helpful to understand the underlying radiation emission process and its impact on the variability of the source.

ACKNOWLEDGMENT

The authors acknowledge the anonymous reviewer for suggestions which improve the quality of the work substantially. HB acknowledges support from Department of Science & Technology INDIA, through INSPIRE faculty fellowship IFA-PH-02. HB further acknowledges R. C. Rannot and R. Koul for their support to work and to pursue DST-INSPIRE position at ApSD, BARC, Mumbai. This research has made use of data obtained from the High Energy Astrophysics Science Archive Research Center (HEASARC), provided by NASA's Goddard Space Flight Center.

REFERENCES

- Abdo A. A. et al., 2009a, ApJ, 707, 727
Abdo A. A. et al., 2009b, ApJL, 707, L142
Arnaud K. A., 1996, in Astronomical Society of the Pacific Conference Series, Vol. 101, Astronomical Data Analysis Software and Systems V, Jacoby G. H., Barnes J., eds., p. 17
Atwood W. B. et al., 2009, ApJ, 697, 1071
Ballantyne D. R., Iwasawa K., Fabian A. C., 2001a, MNRAS, 323, 506
Ballantyne D. R., Ross R. R., Fabian A. C., 2001b, MNRAS, 327, 10
Ballantyne D. R., Vaughan S., Fabian A. C., 2003, MNRAS, 342, 239
Bian W., Zhao Y., 2004, MNRAS, 352, 823
Boller T., Tanaka Y., Fabian A., Brandt W. N., Gallo L., Anabuki N., Haba Y., Vaughan S., 2003, MNRAS, 343, L89
Crummy J., Fabian A. C., Gallo L., Ross R. R., 2006, MNRAS, 365, 1067
Dewangan G. C., Griffiths R. E., Dasgupta S., Rao A. R., 2007, ApJ, 671, 1284

- Done C., Davis S. W., Jin C., Blaes O., Ward M., 2012, MNRAS, 420, 1848
- Edelson R., Turner T. J., Pounds K., Vaughan S., Markowitz A., Marshall H., Dobbie P., Warwick R., 2002, ApJ, 568, 610
- Fabian A. C., Miniutti G., Gallo L., Boller T., Tanaka Y., Vaughan S., Ross R. R., 2004, MNRAS, 353, 1071
- Fabian A. C. et al., 2002, MNRAS, 335, L1
- Foschini L., 2011, in *Narrow-Line Seyfert 1 Galaxies and their Place in the Universe*
- Foschini L. et al., 2012, ArXiv e-prints
- Foschini L., Fermi/Lat Collaboration, Ghisellini G., Maraschi L., Tavecchio F., Angelakis E., 2010, in *Astronomical Society of the Pacific Conference Series, Vol. 427, Accretion and Ejection in AGN: a Global View*, Maraschi L., Ghisellini G., Della Ceca R., Tavecchio F., eds., pp. 243–248
- Foschini L. et al., 2011, MNRAS, 413, 1671
- Gallo L. C. et al., 2006, MNRAS, 370, 245
- Ghisellini G., Tavecchio F., 2009, MNRAS, 397, 985
- Gierliński M., Done C., 2004, MNRAS, 349, L7
- Haba Y., Terashima Y., Kunieda H., Ohsuga K., 2008, *Advances in Space Research*, 41, 174
- Jin C., Ward M., Done C., Gelbord J., 2012, MNRAS, 420, 1825
- Kalberla P. M. W., Burton W. B., Hartmann D., Arnal E. M., Bajaja E., Morras R., Pöppel W. G. L., 2005, A&A, 440, 775
- Laor A., 1991, ApJ, 376, 90
- Laor A., Fiore F., Elvis M., Wilkes B. J., McDowell J. C., 1997, ApJ, 477, 93
- Lyubarskii Y. E., 1997, MNRAS, 292, 679
- Magdziarz P., Blaes O. M., Zdziarski A. A., Johnson W. N., Smith D. A., 1998, MNRAS, 301, 179
- Makishima K., Maejima Y., Mitsuda K., Bradt H. V., Remillard R. A., Tuohy I. R., Hoshi R., Nakagawa M., 1986, ApJ, 308, 635
- McHardy I. M., Papadakis I. E., Uttley P., Page M. J., Mason K. O., 2004, MNRAS, 348, 783
- Mitsuda K. et al., 1984, PASJ, 36, 741
- Nardini E., Fabian A. C., Reis R. C., Walton D. J., 2011, MNRAS, 410, 1251
- Neilsen J., Lee J. C., 2009, *Nature*, 458, 481

- O'Brien P. T., Page K., Reeves J. N., Pounds K., Turner M. J. L., Puchnarewicz E. M., 2001, MNRAS, 327, L37
- Oshlack A. Y. K. N., Webster R. L., Whiting M. T., 2001, ApJ, 558, 578
- Page K. L., O'Brien P. T., Reeves J. N., Breeveld A. A., 2003, MNRAS, 340, 1052
- Papadakis I. E., Brinkmann W., Gliozzi M., Raeth C., Nicastro F., Conciatore M. L., 2010, A&A, 510, A65
- Ross R. R., Fabian A. C., 1993, MNRAS, 261, 74
- Ross R. R., Fabian A. C., 2005, MNRAS, 358, 211
- Strüder L. et al., 2001, A&A, 365, L18
- Sunyaev R. A., Titarchuk L. G., 1980, A&A, 86, 121
- Titarchuk L., 1994, ApJ, 434, 570
- Turner M. J. L. et al., 2001, A&A, 365, L27
- Uttley P., McHardy I. M., 2001, MNRAS, 323, L26
- Uttley P., McHardy I. M., Vaughan S., 2005, MNRAS, 359, 345
- Vaughan S., Edelson R., Warwick R. S., Uttley P., 2003a, MNRAS, 345, 1271
- Vaughan S., Edelson R., Warwick R. S., Uttley P., 2003b, MNRAS, 345, 1271
- Vaughan S., Fabian A. C., Nandra K., 2003c, MNRAS, 339, 1237
- Walton D. J., Reis R. C., Cackett E. M., Fabian A. C., Miller J. M., 2012, MNRAS, 422, 2510
- Yuan W., Zhou H. Y., Komossa S., Dong X. B., Wang T. G., Lu H. L., Bai J. M., 2008, ApJ, 685, 801
- Zdziarski A. A., Gierlinski M., Gondek D., Magdziarz P., 1996, A&AS, 120, C553